Journal of Statistical Physics, Vol. 50, Nos. 5/6, 1988

Morphology of Growing Interfacial Patterns

Debashish Chowdhury[1,2]

Received July 28, 1987

A study is made of the morphology of the interfacial patterns in the solid-on-solid model evolving from initial states very far from equilibrium. Monte Carlo simulation is used to study the time dependence of the length, the diffuseness, and the width of the interface during such evolution in the absence as well as in the presence of quenched random field. Moreover, the technique of Walsh–Fourier transform is introduced for analyzing the noise level in such interfacial patterns. A quantity is also introduced that characterizes the interfacial structure locally on a very short length scale. Finally, the latter technique is also applied to the kinetic Ising model evolving from a random initial configuration.

KEY WORDS: SOS model interfaces; Walsh transform.

1. INTRODUCTION

Formation and growth of fractal patterns[1–3] as well as nonfractal patterns[4] in physical systems has attracted much attention during the last few years. So far as the nonfractal patterns are concerned, theoretical descriptions of the temporal evolution of systems from simple structureless initial states to complex stable (or steady) states or vice versa have been formulated in terms of nonlinear differential equations of motion. Since exact solutions of these nonlinear differential equations are most often unavailable, and since approximations that make analytical solutions possible often miss some of the essential features of the problem, computer simulations have helped enormously in quantitative, albeit approximate, understanding of these phenomena.[5,6] In this paper, using computer simulation techniques, we investigate some new aspects of the formation

[1] Institut für Theoretische Physik, Universität zu Köln, D-5000 Köln 41, West Germany.
[2] Present and permanent address: School of Physical Sciences, Jawaharlal Nehru University, New Delhi 10067, India.

0022-4715/88/0300-1111$06.00/0

of nonfractal ordered structures in freely equilibrating model systems beginning from unstable initial states which are random.[7,8]

The growth of the domains of up (or down) spins in an Ising model following an instantaneous quench from a very high temperature T_h to a low temperature T_l below the coexistence curve is the prototype of the freely equilibrating systems. At least two quantities characterizing such growing patterns have been studied quite extensively. First, the average linear size R of the domains grow with time t according to the Allen–Cahn growth law $R(t) \sim t^{1/2}$ in the kinetic Ising model with nonconserved order parameter (the so-called Glauber dynamics). This *growth law* describes only the rate of growth of the *average* size of the domains in terms of a single characteristic length scale $R(t)$. Moreover, the observation[9] that the structure function has a scaling form implies that the domains are statistically self-similar during the temporal evolution. The curvature invariants[10] go one step further in characterizing these random interfacial patterns. However, despite all the progress in the analysis of the fractal patterns in terms of the various *exponents*, e.g., fractal dimension, spectral dimension, etc., very little attention has been paid to the detailed morphology of growing nonfractal interfacial patterns.

The interfacial instability and pattern selection in diverse physical situations, e.g., directional solidification,[4] viscous fingering in Hele–Shaw cells,[6] has attracted much attention in recent years. Moreover, it has also been realized that the theoretical analysis of the domain growth problems (e.g., that in the kinetic Ising model) is more convenient in terms of the motion of the interfaces separating the different phases.[9–12] In addition, the dynamical evolution of the growing surface profile of the Eden model[13–17] has thrown some light on the morphology of growing surfaces. The recent modeling of growing interfaces by self-avoiding walks[18] also provides insight into certain aspects of interfacial motion. The main aim of this paper is to develop systematic methods of studying the dynamics of interfacial structures in a class of simple growing patterns *with strong emphasis on the morphology*. Most often our discussion will be based on the solid-on-solid (SOS) model as a simple example. We also occasionally concentrate on the kinetic Ising model. The effect of random external fields on the growth of domains from unstable initial states of the Ising model has received some attention during the last few years. The random field tends to pin the interface, thereby slowing down the growth. However, most of the simulations[19–21] have been carried out for the Ising model on discrete lattices, whereas the analytical theories[22–24] have been developed for the simple SOS models. In this paper we study the effects of the random external fields on the time evolution of the SOS model beginning from an initial state far from equilibrium. However, unlike the earlier studies, we not only

study the time dependence of the average domain size, but we also compare and contrast some other aspects of the morphology of the interfacial patterns growing in the presence of random external fields with those growing in the absence of random fields. A short summary of Sections 7 and 8 is being published elsewhere.

2. THE MODELS

Most of our discussions in this paper will be based on two models, the kinetic Ising model and the solid-on-solid (SOS) model.

2.1. The Kinetic Ising Model

The Hamiltonian for the Ising model with nearest neighbor exchange interaction J is given by

$$\mathscr{H} = -J \sum_{\langle ij \rangle} S_i S_j \tag{1}$$

where the Ising spin at the ith site, S_i, can have only two possible values, $+1$ and -1. So far as the dynamical evolution of the system is concerned, we study only the single-spin-flip dynamics, which is also called the Glauber dynamics. The magnetization of the system is not conserved during time evolution.

2.2. The SOS Model

Consider a two-dimensional Ising model with nearest neighbor interactions. The interface separating the up spins from the down spins is a multiple-valued function $z = f(x)$ of x, because of the existence of *droplets* and *overhangs*. Such droplets and overhangs are not allowed in the so-called SOS model, so that the interface $z = f(x)$ is a single-valued function of x. On a discrete d-dimensional lattice the interface is represented as single-valued function $z = f(i)$, where $i = 1, 2, \ldots, N$ is the coordinate labeling the lattice sites in the $(d-1)$-dimensional hyperplane transverse to the z direction. Since droplets and overhangs appear as excitations in the Ising model at not too low temperatures, the SOS model is a good approximation to the Ising model at low temperatures. The *effective Hamiltonian* for the SOS model in d dimensions is given by

$$\mathscr{H} = JN^{d-1} + (J/2) \sum_{\langle ij \rangle} |f(i) - f(j)| \tag{2}$$

where the sum $\langle ij \rangle$ denotes a sum over nearest neighbor columns i and j. It is straightforward to verify that the ground state of the SOS model corresponds to a flat, smooth interface, i.e., $f(i) = \text{const}$ for all i. For all temperatures $0 < T < T_R$, the interface is not flat, but *smooth*, whereas for $T > T_R$ the interface is *rough*. (The width of a rough interface, as opposed to a smooth one, goes to infinity as the interface size goes to infinity.) The temperature T_R is called the roughening temperature. $T_R = 0$ in $d = 2$. Note also that the mathematical simplicity of the SOS model is achieved at the cost of an infinitely large transition temperature, $T_c = \infty$. For the derivation of the *(coarse-grained)* field-theoretic interface Hamiltonians and comparison with the discrete SOS model (2), see the excellent discussion in Ref. 25.

In the presence of random external fields[26] there is an additional term in the Hamiltonian representing the contribution from the interaction of each of the spins S_i with the corresponding local random field H_i, namely $\sum H_i S_i$. From now on we always assume that the distribution of the random local fields H_i is $P(H_i) = 0.5[\delta(H_i - H) + \delta(H_i + H)]$.

3. MONTE CARLO SIMULATION OF THE MODELS

Using Monte Carlo simulation, we investigate the morphology of the patterns in the kinetic Ising model and the SOS model during evolution from random initial states which are far from the corresponding equilibrium configurations. Initially, each of the spins is randomly up or down with equal probability. This random configuration is the equilibrium configuration corresponding to an infinitely high temperature, far from the equilibrium configuration at any finite temperature T. Therefore, the random initial configuration at a finite temperature T is equivalent to quenching the spin system from infinitely high temperature $T_h = \infty$ to a finite low temperature T. The well-known Metropolis updating scheme is used to update the spin configuration. An arbitrary spin is chosen randomly for updating. If the proposed energy change ΔE associated with the spin flip is less than or equal to zero, the spin is *flipped*; otherwise, the *flipping* is carried out with a probability $\exp(-\Delta E/k_B T)$.[27] Updating N spins in an N-spin system constitutes one Monte Carlo step (MCS) per spin. Time is measured in units of MCS. Note that magnetization is not conserved in this dynamical scheme, in contrast to the Kawasaki spin-exchange mechanism, where magnetization is conserved.

So far as the SOS model is concerned, a random initial configuration of $z = f(i)$ $[0 \leqslant f(i) \leqslant M$ for $1 \leqslant i \leqslant N]$ is created using a random number generator. Let us assume that the spins below the interface are all up and those above it are all down. A periodic boundary condition is applied in

the plane transverse to the z direction (from now on the direction transverse to the z direction will be denoted by x for $d=2$). The *flipping* of an Ising spin at $x=k$ just below the interface is equivalent to decreasing $f(k)$ by unity. Similarly, *flipping* an Ising spin at $x=k$ just above the interface is equivalent to increasing $f(k)$ by unity. Since no *droplet* or *overhang* is allowed in the SOS model, only the spins just above and just below the interface are allowed to *flip*. The same Metropolis algorithm is applied also for updating the variables $f(i)$ in the SOS model.[28] Since $\sum f(i)$ is not conserved during the simulation, our algorithm is similar to the Glauber dynamics. Most of our simulations have been carried out in $d=2$.

4. HOW LONG IS THE INTERFACE?

Let us now analyze the morphology of the interface of the SOS model far from the ground state. First, let us focus on the *global* morphological features of the interfacial pattern. The length of the interface $L(t)$ is defined as

$$L(t)=\left\langle N+\sum_{i=1}^{N}|[f(i)-f(i+1)]|\right\rangle \tag{3}$$

where $\langle\cdot\rangle$ denotes average over a large number of quenches.

4.1. Length of the Interface in the Absence of Random Field

In the case of the SOS model we begin with a random initial configuration. As the system evolves with time, the interface *shrinks*. We monitored $L(t)$ as a function of time t (measured in units of MCS/site). We made the following observations (See Fig. 1):

(a) The *growth law* for the interface of the SOS model in the early and intermediate time regimes is

$$L(t)=L(0)(1-\alpha t^{x}) \qquad \text{with} \quad x=1 \tag{4}$$

where α is a constant; this growth law should not be confused with the Allen–Cahn growth law for the kinetic Ising model, because of the basic differences in the two models discussed in Section 2.

(b) The constant α depends on the initial length $L(0)$ of the interface; the larger is $L(0)$, the smaller is the corresponding α.

The interpretation of the observation (b) is quite straightforward. The length of the interface of the SOS model at equilibrium at $T=\infty$ is, in principle, infinite. Therefore, for the SOS model, the larger $L(0)$ value

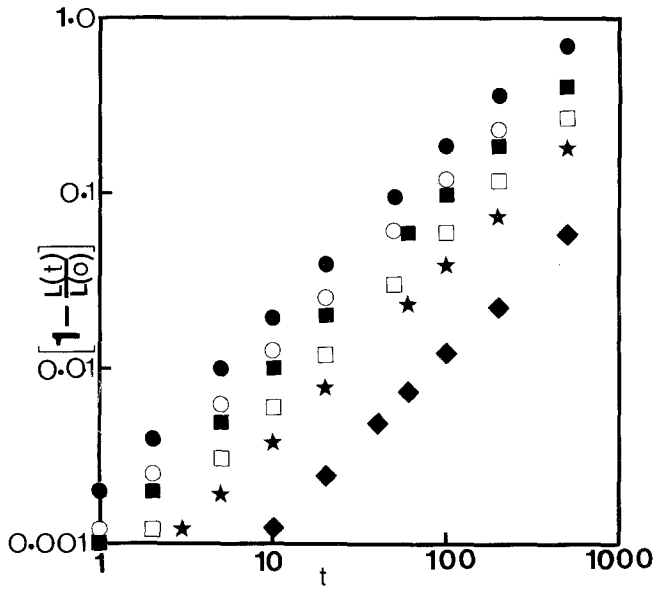

Fig. 1. Log–log plots of $1-L(t)/L(0)$ against t for the two-dimensional SOS model with $N=128$ at various temperatures T for several values of M: (●) $M=2048$, $T=0$; (○) $M=2048$, $T=4.0$; (■) $M=4096$, $T=0$; (□) $M=4096$, $T=4.0$; (★) $M=4096$, $T=8.0$; (◆) $M=32768$, $T=1.0$. Each of the data points was obtained by averaging over 100 quenches.

corresponds to higher T_h. In other words, the smaller is the $L(0)$, the lower is the equivalent T_h. Therefore, finite $L(0)$ for the SOS model at any finite temperature T can be interpreted as a two-stage quench where the first step corresponds to quenching from $T=\infty$ to $T=T_h$; $L(0)$ is the length of the interface at equilibrium at $T=T_h$. The second step of the quenching process corresponds to quenching from $T=T_h$ to the temperature T. The effect of such two-stage quenches on the growth processes have been studied in experiments on intercalated compounds[29] as well as by computer simulation of Q-state Potts model.[30] Both investigations indicated that the growth law for the two-stage quench differs from that for the corresponding one-stage process. Of course, our model is neither exactly equivalent to that of Dasgupta and Pandit, nor can it be applied directly to the experiments of Hommaa and Clarke. Nevertheless, our observation (b) is qualitatively similar to theirs except for the fact that the variation of the quenching procedure affects only the prefactor α and not the exponent x.

(c) In the late stage of temporal evolution, there is a crossover from the linear growth law (4) to a new regime, which we have not investigated in detail.

It is worth mentioning here that the time evolution of the domains in a one-dimensional model of interacting kinks has been analyzed.[31] However, the analytical treatment of this model is much simpler that the two-dimensional SOS model, because the kinks and antikinks must appear alternately in the former, but not necessarily in the latter. Therefore, the dynamical evolution of the interface in the Nagai–Kawasaki model can be described in terms of only three dominating processes, namely creation and annihilation of kink–antikink pairs and drift of the kinks and antikinks. Such a simple description is not possible in the SOS model. The *growth law* proposed by Villain[32] in the context of healing of the rough surface of the terrace–kink–ledge model is quite different from the *growth law* we have observed for the SOS model.

Note that all the qualitative features, including the linear growth of the interface length, are shared by the area of the interface in the three-dimensional SOS model (see Fig. 2).

4.2. Length of the Interface in the Presence of Random Fields

The log–log plots of $1 - L(t)/L(0)$ versus t shown in Fig. 3 exhibit the breakdown of the linear growth law (4) in the presence of quenched

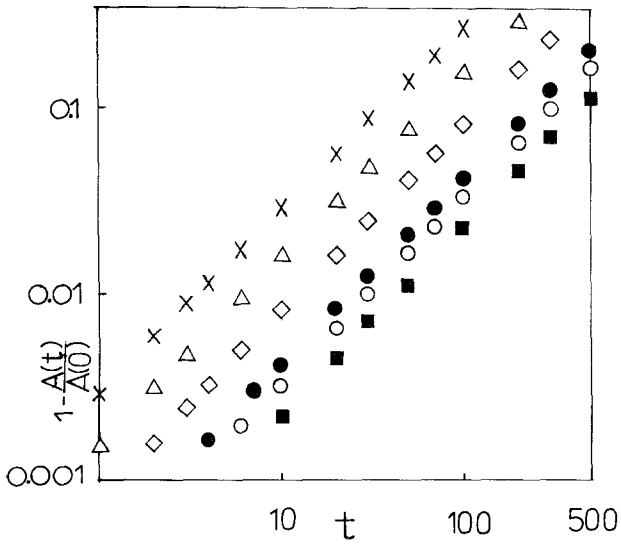

Fig. 2. Log–log plots of $1 - A(t)/A(0)$ against t for the three-dimensional SOS model with $N = 64 \times 64$ at various temperatures T for several values of M: (×) $M = 16$, $T = 0$; (△) $M = 32$, $T = 1.0$; (◇) $M = 64$, $T = 1.0$; (●) $M = 128$, $T = 1.0$; (○) $M = 128$, $T = 4.0$; (■) $M = 128$, $T = 8.0$. Each of the data points was obtained by averaging over 100 quenches.

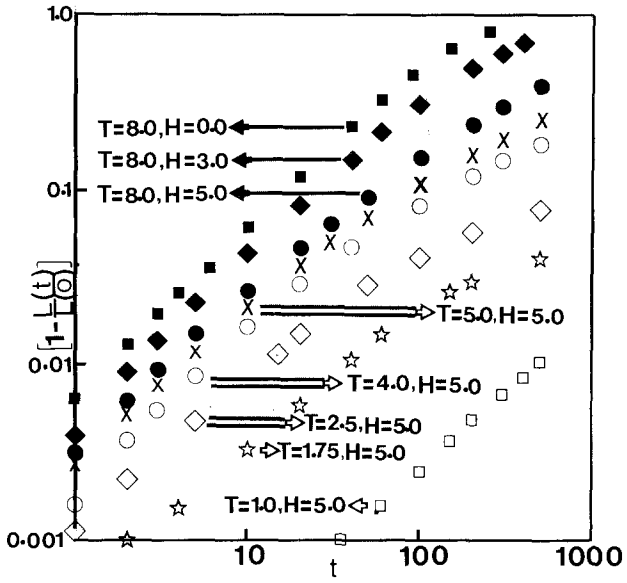

Fig. 3. Log–log plots of $1 - L(t)/L(0)$ against t at various temperatures T for several values of H for the SOS model in the presence of a random field. All the data correspond to $N = 64$ and $M = 230$. Each of the data points was obtained by averaging over 100 quenches.

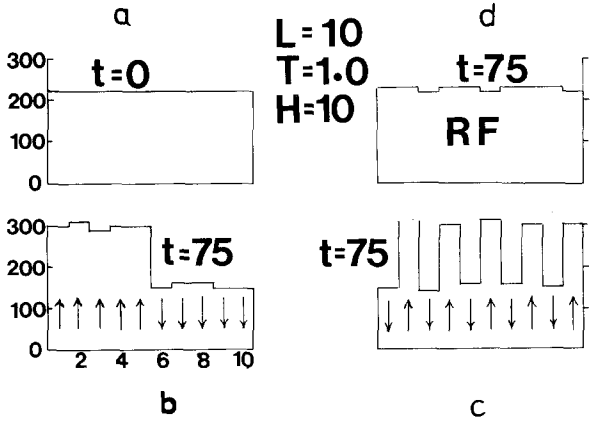

Fig. 4. Typical configurations $f(i)$ of the interface for the SOS model with $N = 10$ corresponding to three different configurations of the quenched field; the local field orientations are shown by the corresponding arrows. (a) The initial flat configuration. (b)–(d). The final configurations corresponding to the three different field configurations.

random fields. First of all, the qualitative nature of the curves for $H \gg T$ is similar to that in the case of the Glauber model in random field.[19,20] Note also that there is a competition between the temperature T and the field H. At a fixed T, the higher is the field, the slower is the evolution. On the other hand, at a fixed H, the higher is the temperature, the faster is the evolution. It seems that the random field pins the interface.

In order to demonstrate the pinning effect of the magnetic field, we consider four simple field configurations, as shown in Fig. 4. Figure 4a shows the interface function $f(i)$, $i = 1,..., 10$, at $t = 0$. Depending on the field configuration, the final (equilibrium) interfaces can be quite different from each other. For example, if the field configuration is $H_i = +H$ for $i = 1,..., 5$ and $H_i = -H$ for $i = 6,..., 10$, then the equilibrium configuration $f(i)$ looks like Fig. 4b. On the other hand, if the field H_i is $+H$ and $-H$ for even i and odd i, respectively, the equilibrium configuration $f(i)$ looks like that shown in Fig. 4c. Finally, for a random field configuration the interface remains more or less pinned at its initial position (Fig. 4d).

5. HOW SHARP (OR SMEARED) IS THE INTERFACE?

Let us illustrate the concept with the SOS model as a simple example, although, more appropriately, it should be applied to models with more complex interfacial structure, e.g., the kinetic Ising model. For a given interface $z = f(i)$, $i = 1,..., N$, we call a site at a height h for $i = k$ *occupied* if $f(k) \geqslant h$, and *empty* otherwise. Let us begin with a random initial configuration for $L = 64$ with $M = 20$. We are interested in the quantity $F(z)$, $z = 0, 1, 2,..., 20$, where $F(h)$ is the fraction of the sites occupied at the level $z = h$. The function $F(z)$ is plotted in Fig. 5 at three intervals of time for two different temperatures. Note that the interface is perfectly sharp after sufficiently long time only at $T = 0$. At all nonzero temperatures the interface is smeared. The width at the half-maximum of $F(z)$ can be taken as a measure of the diffuseness of the interface. However, note that a *smeared* interface does not neccessarily imply a rough interface. The usual measure of the roughness of an interface will be mentioned in the next section.

6. HOW WIDE IS THE INTERFACE?

The width of the interface $W(t)$ at time t is defined by

$$W(t) = \left\{ \left\langle (1/N) \sum_{i=1}^{N} [f(i, t) - f_m(t)]^2 \right\rangle \right\}^{1/2}$$

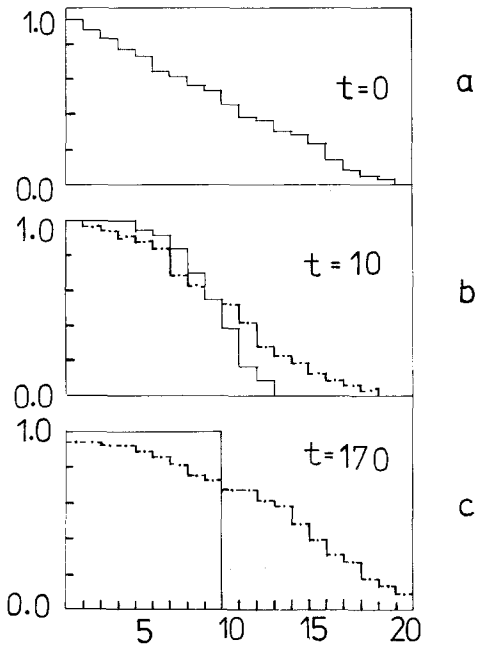

Fig. 5. The function $F(h)$ (see the text for the definition) in the SOS model with $N=64$, $M=20$ for three successive instants of time: $t=0$, 10, and 170. (—) $T=0$; (- - -) $T=8.0$. Note that at $T=0$, the final configuration at $t=170$ is a step function because the interface is flat in equilibrium.

where $f_m(t)=(1/N)\sum f(i,t)$ is the mean position of the interface at time t and the brackets $\langle\cdot\rangle$ denote average over a large number of quenches.[28] In other words, the width $W(t)$ is the root-mean-square height of the interface measured from the mean position of the interface at time t. Note that two equally wide configurations of the interface in the SOS model can have different lengths, as shown in Figs. 6a and 6b. The width of growing interfaces of several different types of patterns has attracted attention over the last few years. The relation between the $W(t)$ and N for an SOS model defines the *roughness* of the interface; if W diverges with increasing N, the interface is called rough.

6.1. Width of the Interface of the SOS Model in the Absence of Random Field

The time dependence of $W(t)$ for the SOS model with finite size is shown in Fig. 7. The nonexponential decay is consistent with similar earlier observations for the Gaussian model.[33]

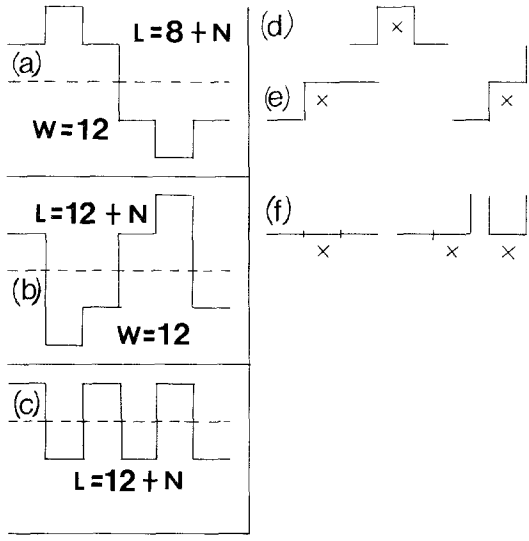

Fig. 6. (a)–(c) Three finite segments of the interface in the SOS model. The interfaces in (a) and (b) have the same width, but different lengths. The interfaces in (b) and (c) are equally long, but the one in (c) is more *regular* than that in (b). (d)–(f) Some typical sites, marked by the crosses, along the interface of the SOS model with three dissimilar neighbors, two dissimilar neighbors, and one dissimilar neighbor, respectively.

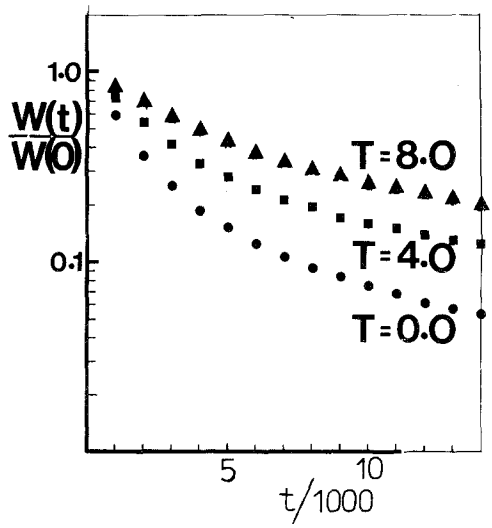

Fig. 7. Semilog plots of $W(t)/W(0)$ against t for the SOS model with $N=1024$ and $M=4096$ at three different temperatures T. Each of the data points was obtained by averaging over ten quenches.

6.2. Width of the Interface of the SOS Model in the Presence of Random Field

The time dependence of the interface in the presence of the random field is shown in Fig. 8 for several different values of H and T. Because of the pinning tendency of the random field, the lower is the temperature, the wider is the interface at a given time t.

7. HOW NOISY IS THE INTERFACE?

An interface may be very regular (not necessarily flat) or irregular. For example, the interface shown in Fig. 6c is perfectly regular, whereas that in Fig. 6b is irregular, although both these interfaces have equal lengths. The question we pose in this section is: how *irregular* or *noisy* is an interface at a given instant of time during its evolution? In order to answer this question, we need a unique definition of the amount of *noise* in an interfacial pattern.

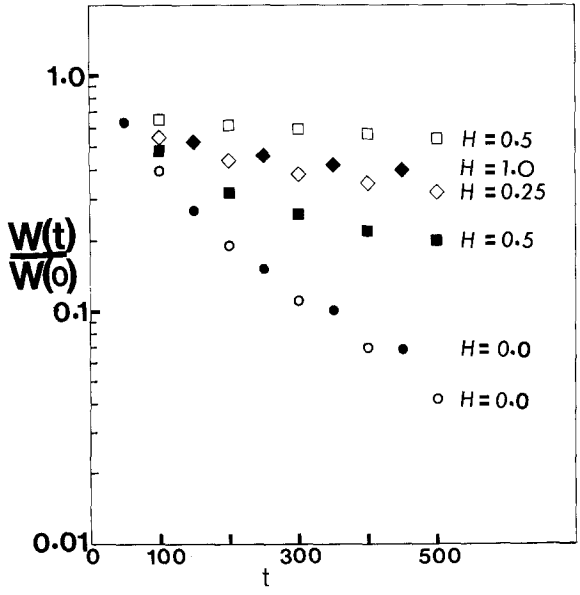

Fig. 8. Semilog plots of $W(t)/W(0)$ against t for the SOS model with $N=64$, $M=230$ for different values of H and T. The empty symbols correspond to $T=0.25$, whereas the filled symbols correspond to $T=1.0$. Each of the data points is obtained by averaging over 100 quenches.

7.1. Noise in an Interface. A Real-Space Description

We have computed the distribution $P(\Delta f)$ of the quantity $\Delta f = 2f(x, t) - f(x+1, t) - f(x-1, t)$ for all x as a function of time t. The broader and denser is the distribution $P(\Delta f)$, the noisier is the interface (a more precise definition of the noise level in an interface will be given in the next subsection). The distribution $P(\Delta f)$ is shown in Fig. 9 at increasing values of time t. Note that $P(\Delta f)$ narrows down with the increase of time t; the higher is the temperature, the slower is the narrowing. However, there is a fundamental difference between the nature of $P(\Delta f)$ at time $t = \infty$ for $T = 0$ and that for $T > 0$. Since the interface is not flat at finite T even at $t = \infty$, $P(\Delta f) \to \delta(\Delta f)$ as $t \to \infty$ only at $T = 0$.

7.2. Noise in an Interface. A Fourier-Space Description

Before defining a measure of the noise in an interface, let us describe the Fourier method of analyzing the structure of an interface. In the

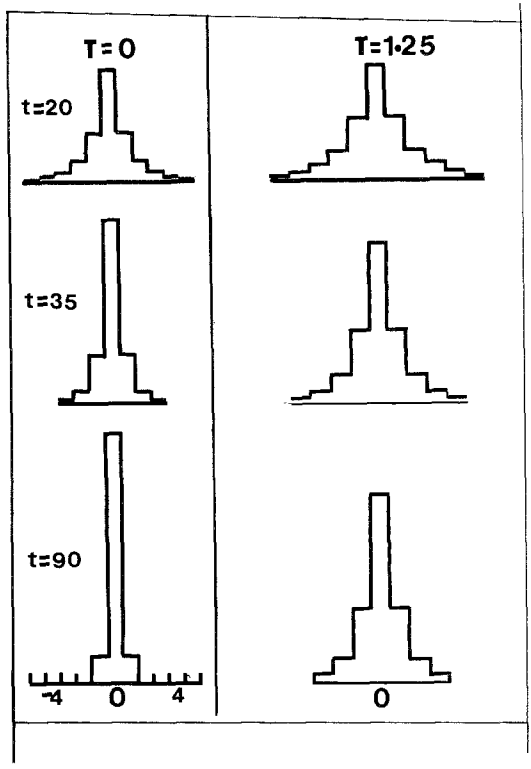

Fig. 9. The distribution $P(\Delta f)$ (see the text for the definition) at times $t = 20$, 35, and $t = 90$ corresponding to two different temperatures $T = 0$ and 1.25.

continuum (field) theories an interface at time t is defined as a function $f(x; t)$, where x describes the continuum. The Fourier expansion of the function $f(x; t)$ is given by

$$f(x; t) = \sum_k c_k(t) \exp(ikx)$$

Therefore, the time evolution of the interface $f(x; t)$ can be described in terms of the corresponding time evolution of the Fourier coefficients $c_k(t)$.[34] Now we can define a measure of the noise level in an interfacial pattern. The larger is the number of plane wave *modes* with nonzero amplitudes c_k, the noisier is the interface.

Let us now generalize the Fourier transform method appropriately for the discrete model (1). Our numerical technique is an extension of some of the conventional techniques used in the field of pattern recognition. Since computer simulations as well as other numerical investigations are carried out on a discrete lattice, it is more convenient to use the generalized Fourier transforms (in this case Walsh–Fourier transform) where the exponential functions $\exp(ikx)$ are replaced by the Walsh functions.[35,36] The Walsh–Fourier transform of a function $f(x; t)$ is given by

$$f(x; t) = \sum_k a_k(t)\, D_k(x)$$

where $D_k(x)$ $(k = 0, 1, 2,...)$ are the Walsh functions defined over the interval $-1/2 \leqslant x \leqslant 1/2$. Therefore, the time evolution of the interface on a discrete lattice can be described by the corresponding time evolution of the Walsh coefficients $a_k(t)$. In order to define the Walsh functions, let us introduce the operation symbolized by $\oplus$. Let m and n be two integers. Then the operation $m \oplus n$ consists of the following steps: (a) Write m and n in the binary notation, and (b) add their corresponding digits using the modulo 2 arithmetic (logical operation EXCLUSIVE-OR). The modulo 2 rule for summation is $0 \oplus 1 = 1 \oplus 0 = 1$ and $0 \oplus 0 = 1 \oplus 1 = 0$. Thus, $5 \oplus 1 = 101 \oplus 001 = 100 = 4$. The Walsh functions $D_k(x)$ $(k = 0, 1,...)$ are defined by $D_0(x) = 1$ for all $-1/2 \leqslant x \leqslant 1/2$:

$$D_1(x) = \text{sign}(\sin \pi x)$$

$$D_p(x) = \text{sign}(\cos p\pi x), \qquad p = 2^n \ (n > 0)$$

$$D_{m \oplus n}(x) = D_m(x)\, D_n(x)$$

For example,

$$D_7(x) = D_4(x)\, D_2(x)\, D_1(x), \qquad D_{12}(x) = D_{10}(x)\, D_6(x).$$

Walsh–Fourier transform is particularly convenient for functions $f(x)$ that are stepwise discontinuous functions on 2^q intervals. Let us consider the SOS model with $L=8$, so that the height of the interface $f(x)$ is a stepwise discontinuous function over 2^q intervals with $q=3$. The interval of x can be squeezed or stretched within the interval $(-1/2, 1/2)$, so that the x coordinates of the eight points $i=1, 2,..., 8$ are $x=-1/2$, $-3/8$, $-1/4$, $-1/8$, $1/8$, $1/4$, $3/8$, and $1/2$, respectively. The corresponding Walsh functions are shown in Fig. 10. The Walsh functions $D(x)$ are related to the Sal functions $DS(x)$ and Cal functions $DC(x)$[36] by the relations

$$DS_n(x)=D_{2n-1}(x), \qquad DC_n(x)=D_{2n}(x)$$

Note that Sal and Cal functions are the analogues of the sine and cosine functions, respectively. The fits of Sal and Cal functions with the corresponding sine and cosine functions are particularly good for the higher values of n.

We have monitored the time dependence of the Walsh coefficients of the interface of the SOS model with $N=8$. Some of these coefficients are shown in Fig. 11. Note that the interface of the SOS model is flat at $t=\infty$ only for $T=0$. Therefore, $a_0(\infty)=1$ only at $T=0$. Similar analysis of the noise level in a two-dimensional interface of the three-dimensional SOS

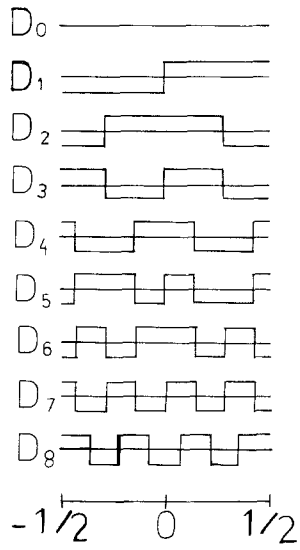

Fig. 10. The Walsh functions $D_k(x)$, $k=0, 1, 2,..., 8$, within the interval $-1/2 \leqslant x \leqslant 1/2$. Note that the larger is k, the closer is the $D_k(x)$ to the corresponding sine function.

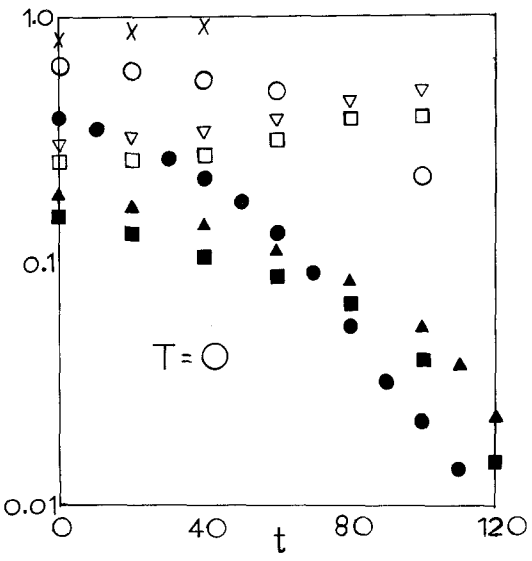

Fig. 11. The Walsh coefficients a_2, a_3, and a_6 for the SOS model at $T=0$ with $N=8$. The open symbols correspond to $M=265$, the closed symbols to $M=256$ (the crosses denoting a_0). Note that the heights were measured with respect to the mean height to obtain the open symbols, and therefore the corresponding a_0 were zero at all t.

model can also be carried out using the two-dimensional Walsh functions[35] $D_{mn}(x, y) = D_m(x)\, D_n(y)$.

The flattening of sinusoidal grooved crystal surfaces has been studied theoretically and experimentally as well as by computer simulation over the last three decades.[32,37–43] However, our model does not describe these experimental situations, not only because the initial interface is far from sinusoidal, but also because we neglect surface and bulk diffusion processes. However, we emphasize that our model can be generalized to incorporate these physical processes, and our basic techniques for analyzing the morphology can be used also for such generalized models.

8. OCCUPATION OF THE *LOCAL* ENERGY LEVELS BY THE INTERFACIAL SPINS

Let us now focus on some *local* properties of the interface. Most of the methods described above characterize the morphology of the interface on a length scale much longer than the nearest neighbor distance. Of course, the analysis in terms of the Walsh functions probes the interface on a range of length scales, the smallest being the distance between the zeros of $D_{\max}(x)$, where $a_k = 0$ for all $k > k_{\max}$. In this section we describe a simple method

based on the *local* structure of the interface. In any pattern consisting of two different types of *species* one individual member of one of the species may have neighbors belonging to the other species. Under those circumstances one can use a simple method for characterizing the morphology of the patterns during growth. For example, the morphology of the growing patterns during phase separation in binary alloys (Ising model on a discrete lattice with Kawasaki spin-exchange dynamics) can be described by the fraction of sites $C_n(t)$ with n *dissimilar* beighbors. In case of the Ising model on a square lattice, n can vary from $n=0$ to $n=4$. So far as only the sites along the interface of the SOS model are concerned, n varies between 1 and 3. We consider only the topmost sites of each column just below the interface. Some typical configurations corresponding to $n=1, 2$, and 3 are shown in Figs. 6d–6f. Accordingly, the interfacial sites can be in one of the three energy levels $(2n\text{-}4)$ J. Similar concepts have been utilized[44] for characterizing the crystal-vapor interface in terms of the "distribution of atoms over the surface energy levels."

The time dependence of $C_n(t)$ for the SOS model and the kinetic Ising model is shown in Figs. 12 and 13. Note that in this analysis we have not

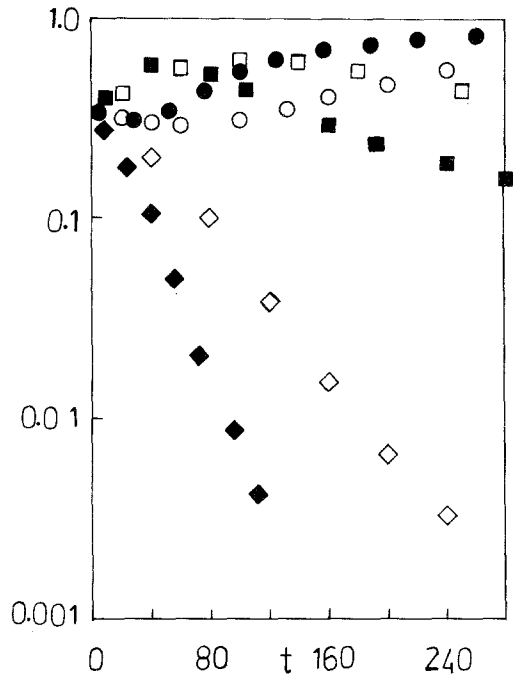

Fig. 12. The fractions $C_1(t)$, $C_2(t)$, and $C_3(t)$ for the SOS model at $T=0$ with $N=512$. The closed symbols correspond to $M=128$, the open symbols to $M=256$.

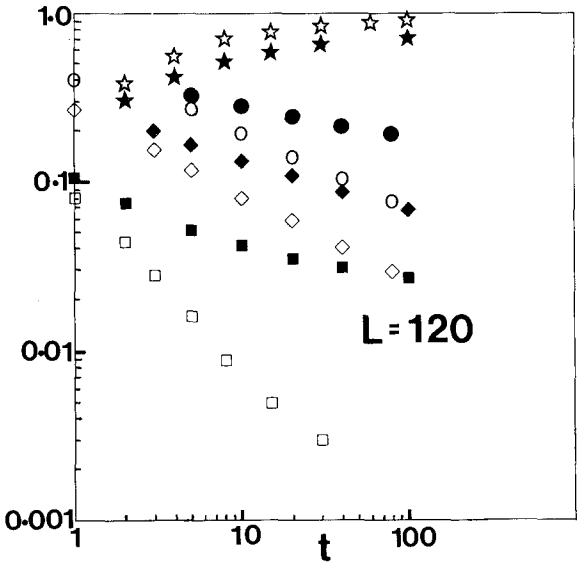

Fig. 13. The log–log plots of $C_n(t)$ against t for the kinetic Ising model. Stars, circles, diamonds, and squares correspond to C_0, C_1, C_2, and C_3, respectively. The empty symbols correspond to $T = 0.45T_c$ and the filled symbols to $T = 0.9T_c$, where $T_c = 2.269$ is the transition temperature of the two-dimensional Ising model. Each of the data points is obtained by averaging over 100 quenches of systems with linear size $L = 120$.

distinguished between the different *geometric* structures of the interface for a given n. Since occupation of these local energy levels is likely to be governed by the Boltzmann distribution, an exponential decay of the coefficients $C_n(t)$ would be expected. Our numerical data also seem to indicate an exponential decay of these coefficients.

9. SUMMARY AND CONCLUSION

Using the Monte Carlo simulation technique, we have computed several different quantities for characterizing the morphology of the growing interfacial pattern in one of the simplest models of interface, namely the SOS model. Some of these quantities are generalizations of older concepts in the literature. We have introduced some new concepts, e.g., the Walsh–Fourier transform, into the field of statistical physics. These quantities, or suitable generalizations, can be used to characterize the corresponding patterns in more complex systems.

So far as the theoretical models of interfaces are concerned, the validity of the continuum interface Hamiltonians[45–48] is limited to length

scales large enough so that $\langle |\nabla f|^2 \rangle$ is small compared to unity.[25] On the other hand, in this work we have investigated the interface on all length scales between the lattice constant and the linear size of the system. Therefore, we cannot represent the interface during the early as well as intermediate stages of evolution by the continuum models obtained by "coarse-graining" the discrete interfaces. The continuum models describe "gently curved" interfaces and therefore may be applicable only to the late stages of evolution.

ACKNOWLEDGMENTS

It is my great pleasure to thank Dietrich Stauffer, Walter Selke, Dietrich Wolf, Janos Kertesz, and Jim Gunton for useful discussions. I also thank Dietrich Stauffer for a critical reading of the manuscript and Indrani Chowdhury for her assistance in drawing some of the figures. The author is an Alexander von Humboldt Fellow.

REFERENCES

1. H. E. Stanley and N. Ostrowsky, eds., *On Growth and Form: Fractal and Nonfractal Patterns in Physics* (Martinus Nijhoff, Dordrecht, 1986).
2. L. Pietronero and E. Tosatti, eds., *Fractals in Physics* (North-Holland, Amsterdam, 1986).
3. H. J. Herrman, *Phys. Rep.* **136**:153 (1986).
4. J. S. Langer, *Rev. Mod. Phys.* **52**:1 (1980).
5. K. Binder and D. Stauffer, *Adv. Phys.* **25**:343 (1976).
6. D. Bensimon, L. P. Kadanoff, S. Liang, B. Shraiman, and C. Tang, *Rev. Mod. Phys.* **58**:1977 (1986).
7. J. D. Gunton, M. San Miguel, and P. S. Sahni, in *Phase Transition and Critical Phenomena*, Vol. 8, C. Domb and J. L. Lebowitz, eds. (Academic Press, 1983); see also J. L. Lebowitz, J. Marro, and M. H. Kalos, *Acta Metall.* **30**:297 (1983).
8. J. D. Gunton and M. Droz, *Introduction to the Theory of Meta-Stable and Unstable States* (Lecture Notes in Physics, Vol. 183, Springer, Berlin, 1983).
9. T. Ohta, D. Jasnow, and K. Kawasaki, *Phys. Rev. Lett.* **49**:1223 (1982).
10. H. Tomita, *Prog. Theor. Phys.* **76**:952 (1986).
11. S. M. Allen and J. W. Cahn, *Acta Metall.* **27**:1017, 1085 (1979).
12. K. Kawasaki, *Phys. Rev. A* **31**:3880 (1985).
13. M. Plischke and Z. Racz, *Phys. Rev. A* **32**:3825 (1985).
14. M. Kardar, G. Parisi, and Y. C. Zhang, *Phys. Rev. Lett.* **56**:889 (1986).
15. J. G. Zabolitzky and D. Stauffer, *Phys. Rev. A* **34**:1523 (1986).
16. R. Hirsch and D. E. Wolf, *J. Phys. A* **19**:L251 (1986).
17. D. E. Wolf and J. Kertesz, *J. Phys. A* **20**:L257 (1987); D. E. Wolf and J. Kertesz, *Europhys. Lett.* (1987); J. Kertesz and D. E. Wolf, Preprint (1987).
18. D. Stauffer and N. Jan, Preprint (1987).
19. E. T. Gawlinski, K. Kaski, M. Grant, and J. D. Gunton, *Phys. Rev. Lett.* **53**:2286 (1984).
20. D. Chowdhury and D. Stauffer, *Z. Phys. B* **60**:249 (1985); see also S. R. Anderson, Preprint (1987).

21. E. Pytte and J. F. Fernandez, *Phys. Rev. B* **31**:616 (1985).
22. M. Grant and J. D. Gunton, *Phys. Rev. B* **29**:1521, 6266 (1984).
23. G. Grinstein and J. F. Fernandez, *Phys. Rev. B* **29**:6389 (1984).
24. J. Villain, *Phys. Rev. Lett.* **52**:1543 (1984).
25. D. A. Huse, W. van Saarloos, and J. D. Weeks, *Phys. Rev. B* **32**:233 (1985).
26. Y. Imry, *J. Stat. Phys.* **34**:849 (1984); G. Grinstein, *J. Appl. Phys.* **55**:2371 (1984); J. Villain, in *Scaling Phenomena in Disordered Systems*, R. Pynn, ed. (Plenum, New York, 1986).
27. K. Binder and D. Stauffer, in *Applications of the Monte Carlo Methods in Statistical Physics*, 2nd ed., K. Binder, ed. (Springer, Berlin, 1987).
28. R. H. Swendsen, *Phys. Rev. B* **15**:5421 (1977).
29. H. Homma an R. Clarke, *Phys. Rev. Lett.* **52**:629 (1984).
30. C. Dasgupta and R. Pandit, *Phys. Rev. B* **33**:4752 (1986).
31. T. Nagai and K. Kawasaki, *Physica* **121A**:175 (1983).
32. J. Villain, *Europhys. Lett.* **2**:531 (1986).
33. H. Müller-Krumbhaar, *Z. Phys. B* **25**:287 (1976).
34. S. Sarkar and M. H. Jensen, *Phys. Rev. A* **35**:187 (1987), and references therein.
35. E. A. Lord and C. B. Wilson, *The Mathematical Description of Shape and Form* (Ellis Horwood, England, and Halsted Press, New York, 1984).
36. H. F. Harmuth, *Transmission of Information by Orthogonal Functions* (Springer, Berlin, 1972).
37. C. Herring, *J. Appl. Phys.* **21**:301 (1950).
38. W. W. Mullins, *J. Appl. Phys.* **30**:77 (1959).
39. P. S. Maiya and J. M. Blakely, *J. Appl. Phys.* **38**:698 (1967).
40. J. M. Blakely, *Introduction to the Properties of Crystal Surfaces* (Pergamon Press, 1973).
41. K. Hoehne and R. Sizman, *Phys. Stat. Sol.(a)* **5**:577 (1971).
42. G. Martin and B. Perraillon, *Surf. Sci.* **68**:57 (1977).
43. W. Selke, *J. Phys. C* **20**:*L*455 (1987).
44. H. J. Leamy and K. A. Jackson, *J. Appl. Phys.* **42**:2121 (1971).
45. F. P. Buff, R. A. Lovett, and F. H. Stillinger, *Phys. Rev. Lett.* **15**:621 (1965).
46. D. J. Wallace and R. K. P. Zia, *Phys. Rev. Lett.* **43**:808 (1979).
47. H. W. Diehl, D. M. Kroll, and H. Wagner, *Z. Phys. B* **36**:329 (1980).
48. K. Kawasaki and T. Ohta, *Prog. Theor. Phys.* **67**:147 (1982).